AD_____

Award Number:
W81XWH-11-1-0042

TITLE:
Improvements in Diagnostic Accuracy with Quantitative Dynamic Contrast-Enhanced MRI

PRINCIPAL INVESTIGATOR:
Federico Pineda

CONTRACTING ORGANIZATION:
The University of Chicago
Chicago, IL 60637-5418

REPORT DATE:
March 2014

TYPE OF REPORT:
Annual Summary

PREPARED FOR: U.S. Army Medical Research and Materiel Command
                        Fort Detrick, Maryland 21702-5012

REPORT DOCUMENTATION PAGE

1. REPORT DATE	2. REPORT TYPE	3. DATES COVERED
March 2014	Annual Summary	1 Dec 2010 – 30 Nov 2013

4. TITLE AND SUBTITLE

Improvements in Diagnostic Accuracy with Quantitative Dynamic

Contrast-Enhanced MRI

5a. CONTRACT NUMBER

5b. GRANT NUMBER
W81XWH-11-1-0042

5c. PROGRAM ELEMENT NUMBER

6. AUTHOR(S)

Federico Pineda, Gregory Karczmar, Ph.D.

email: fdp@uchicago.edu

5d. PROJECT NUMBER

5e. TASK NUMBER

5f. WORK UNIT NUMBER

7. PERFORMING ORGANIZATION NAME(S) AND ADDRESS(ES)

The University of Chicago

Chicago, IL 60637-5418

8. PERFORMING ORGANIZATION REPORT NUMBER

9. SPONSORING / MONITORING AGENCY NAME(S) AND ADDRESS(ES)
U.S. Army Medical Research and Materiel Command
Fort Detrick, Maryland 21702-5012

10. SPONSOR/MONITOR'S ACRONYM(S)

11. SPONSOR/MONITOR'S REPORT NUMBER(S)

12. DISTRIBUTION / AVAILABILITY STATEMENT
Approved for Public Release; Distribution Unlimited

13. SUPPLEMENTARY NOTES

14. ABSTRACT

Scanning of patients with a research acquisition protocol and calibration phantoms has continued. We identified the major sources of variability and error in our quantitative analysis. B1, or transmit field, inhomogeneity is a large source of error in the estimation of concentration of contrast media. To account for this we have developed a method using fat as a reference signal to correct for spatial variations in the B1 field. Further analysis of patients scanned repeatedly at 1.5T and 3T had identified that parameters related to the shape of the signal enhancement versus time curves during DCEMRI of lesions show relatively low variability. Analysis of all the cases acquired to date with the refined methods is underway.

15. SUBJECT TERMS: `none listed`

16. SECURITY CLASSIFICATION OF:			17. LIMITATION OF ABSTRACT	18. NUMBER OF PAGES	19a. NAME OF RESPONSIBLE PERSON USAMRMC
a. REPORT	b. ABSTRACT	c. THIS PAGE			
U	U	U	UU	15	19b. TELEPHONE NUMBER *(include area code)*

Table of Contents

Introduction

We propose to develop methods that allow for the acquisition of truly quantitative images of a dynamic contrast-enhanced (DCE) MRI of the breast. To achieve this we have developed novel calibration phantoms consisting of compartments with varying amounts of contrast agent. The phantoms provide a reference signal that can be used to convert signal enhancement to a measure of the concentration of the contrast media in tissue, as well as quantitative proton density images of the breast. These quantitative images allow for standardized analysis of the DCE-MRI data, leading to diagnostically useful parameters derived from pharmacokinetic modeling of the data. We are investigating whether these parameters will aid in determining malignancy. We will also determine whether our methods reduce variability in the enhancement patterns seen across different scanners and field strengths, providing a way to standardize clinical DCE-MRI data, which would allow for inter-institutional comparisons and comparisons of different scans of the same patient. We are investigating the potential of non-surgical management of high risk breast lesions with MRI, by scanning patients with biopsy proven lesions that carry an increased risk of being associated with a malignancy. Our goal is to determine whether clinical interpretation, semi-quantitative and full quantitative analysis of these images can safely rule out malignancies, an outcome that would help reduce the number of surgeries of these lesions in the future. Finally, we believe MRI-detectable proton density may prove to be a novel and useful biomarker for the detection of breast cancer.

Body

In the period encompassing December 2012 to January 2014, 20 patients were scanned with the full research protocol, including the calibration phantoms previously described. This brings the total to 62 patients scanned. The research protocol consists of: a coil sensitivity scan, a variable flip angle (VFA) sequence (TR = 10ms, FA's = 5, 10, 15, and 20°; TR =25ms, FA's = 5, 15°), a T2-weighted scan, a T1-weighted, fat suppressed, spoiled gradient echo sequence with short TR and TE before (2-3 acquisitions) and after (5-7) a 0.1mM/kg injection of contrast media at an injection rate of 2ml/s. Our collaborators at NorthShore University Healthsystem in Evanston, IL, have scanned a total of 31 patients presenting with high-risk breast lesions, our acquisition protocols were standardized. However scans at NorthShore did not include our calibration phantoms.

In a previous report we described large variations in MRI apparent proton density (M0) results; likely due to the relatively short repetition time (10ms) of the variable flip angle sequence, combined with the long T1 values of some voxels. We attempted to combine the 10ms and 25ms VFA data to refine the estimated M0 and T1 values for each voxel. This, however, proved to be difficult and did not yield better estimates of these values. A possibility for this is that the rescaling of the exported data did not entirely account for changes in the gain, and due to time constraints in the research scans the volume of the 25ms VFA acquired was smaller than the VFA volume and due to this the lesion was not always covered by the 25ms acquisition. A

second approach, using the signal from the phantom compartments to provide a reference for proton density values and creating bounds on the VFA fits for tissue voxels was also explored, unfortunately, it yielded unsatisfactory results. One likely reason for this is the fact that correction for inhomogeneity in the B1 or transmit field were not performed. We are in the process of developing a new method for T1 estimation based on a reference signal present in the VFA, which could be fat voxels or the signal in the calibration phantoms. In this approach the product of the ratio of signals at two different flip angles is used to find T1, using an signal from a region with a previously known T1 it is possible to find an expression for the T1 of the voxel of interest that depends only on the reference T1, TR, and the flip angles used, eliminating the dependence on M0. Simulations have shown the feasibility of this method. However knowledge of the actual flip angles, and thus the B1 field is critical for this method to provide accurate estimates of T1.

Conversion from signal intensity to concentration of contrast media was performed with a reference signal model proposed by Medved et al. (1), previously described. This is a linear method which relies on the fact that under certain conditions the product of signal times T1 is relatively constant. Compartments from the calibration phantoms were used to provide the reference signal. Issues with the pharmacokinetic analysis described in a previous report caused us to re-visit the assumptions in the derivation of the linear reference signal model. We discovered that due to the flip angle of the dynamic contrast enhanced (DCE) portion of the examination, which was 12°, the estimated concentration from the linear model would be lower (in some cases significantly) than the actual concentration, see Figure 1. Simulations showed that the linear model is only adequate when the flip angle used for the acquisition is greater than 60°. This means that the adequate model to use for estimation of concentration of contrast media is the non-linear solution to the spoiled gradient echo signal model (2). Uncertainty analysis on the non-linear method, following the formalism proposed by Schabel et al. (3), and using the acquisition parameters from our scans, show that this solution is very sensitive to uncertainties in the flip angle, i.e. B1 inhomogeneity (Figure 2). An alternative to this is an expanded reference signal model that does not use a high flip angle approximation. Simulations showed that such an expanded model also has a high sensitivity to the actual flip angle. Additionally, this model still has a dependence of the ratio of MRI detectable proton density between tissues and the phantom compartment. Due to these issues estimation of concentration for all the cases acquired concentration will be estimated using the non-linear analytic solution to gradient echo signal model, using native tissue T1s from the VFA data.
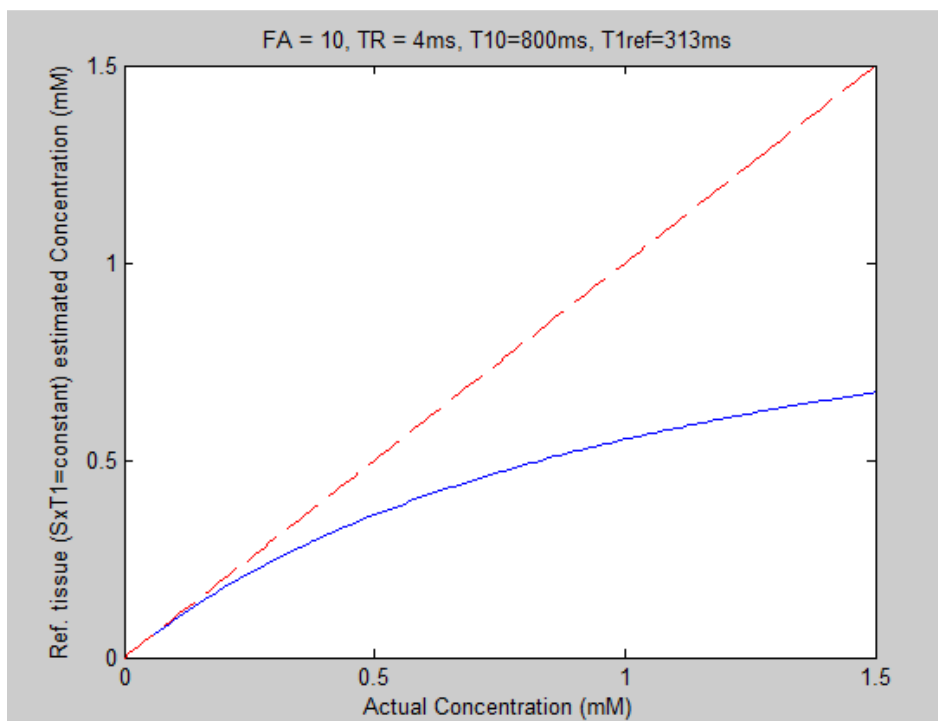
Figure 1. Actual concentration vs estimated concentration for the linear reference signal model when DCEMRI is acquired with a 'low' Flip Angle

As we have stated knowledge of the flip angle at each location in the breast is necessary for an accurate estimate of native T1 and concentration of contrast media, especially when using the non-linear solution to the signal model. Previous work by groups using scanners and coils from the same vendor have shown significant variations in the B1 fields across the field of view (4)(5). This requires the acquisition of a B1 (transmit field) map for each case. As stated in a previous report, we attempted to acquire B1 maps using the actual flip angle imaging method proposed by Yarnykh (6). Our initial attempts to acquire B1 maps with this method were unsuccessful. Since then we have modified the acquisition parameters, increasing the voxel sizes, repetition times and flip angles, and have found better results. However even with the new acquisition parameters we have still seen some dependence in the resulting map on native T1. It is possible that incomplete spoiling of the transverse magnetization could be affecting the accuracy of the resulting maps (7). We continue to improve our acquired B1 maps using this technique.
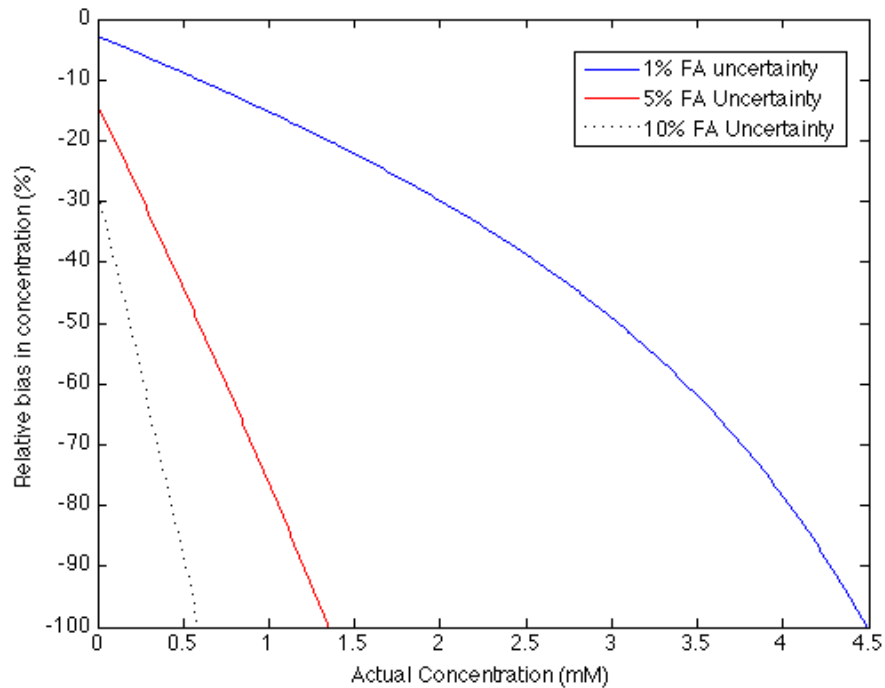
Figure 2. Relative bias in estimated concentration with the non-linear method as a result of three different levels of B1 uncertainty

However this does not solve the issue for cases acquired previously. To solve this issue we have developed and tested a method based on the T1 of adipose tissue in the breast. The premise of this method is the assumption that the T1 of fat is uniform throughout the breast and intra-patient variations in fat T1 values are relatively small. Published results of fat T1 in the breast show a small standard deviation, at 3T they found T1 = 366.78 ± 7.75ms (8). The small standard deviation across patients indicates it is reasonable to assume that the T1 value of fat in different patients will not vary widely. In addition, we have developed a protocol to accurately measure the T1 value of fat in patients. A single voxel spectroscopic (PRESS) inversion recovery series with 4 inversion times was acquired. Our results so far have fallen in line with what was reported by Rakow-Penner et al. A T1 value for all fat voxels can also be calculated with the VFA series acquired before the injection of contrast media. Deviations between the VFA T1 value and the true fat T1 can be attributed to spatial variations of the actual flip angle. By correcting for the location of the Ernst angle (the angle at which the gradient echo signal is maximum) it is possible to find a flip angle correction factor for each voxel by solving the following expression.

$$A = \frac{\cos^{-1}\left(e^{-\frac{TR}{T_{1,t}}}\right)}{\cos^{-1}\left(e^{-\frac{TR}{T_{1,m}}}\right)}$$

Where $T_{1.t}$ is the true T1 value, and $T_{1.m}$ is the measured T1 value. The correction factor 'A' can be calculated for all the fat voxels present in a slice giving us a partial B1 map (Figure 3). This method has also been tested in a (uniform) flood phantom where the T1 can be accurately measured (Figure 4).
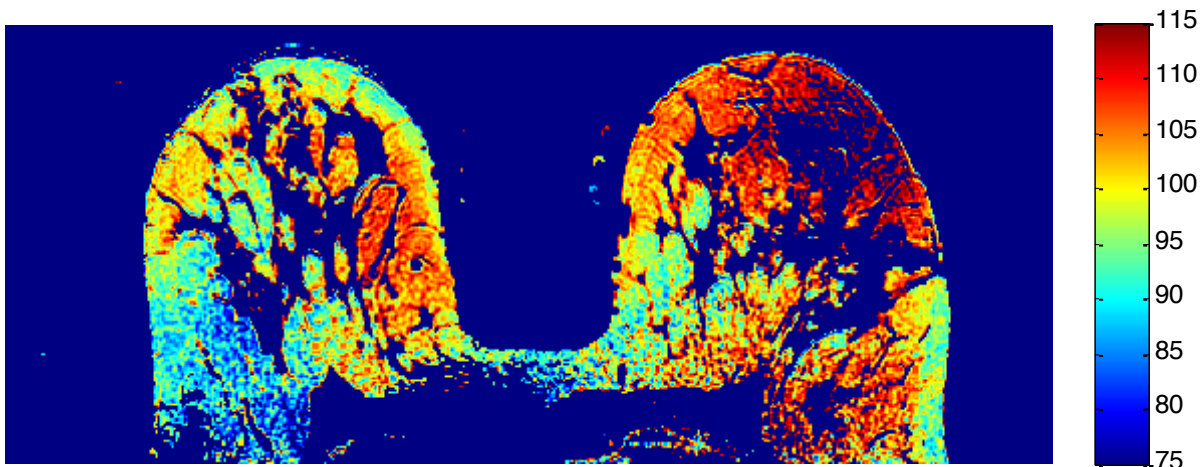
Figure 3. Percent flip angle correction factor for fat voxels found correcting VFA T1 values
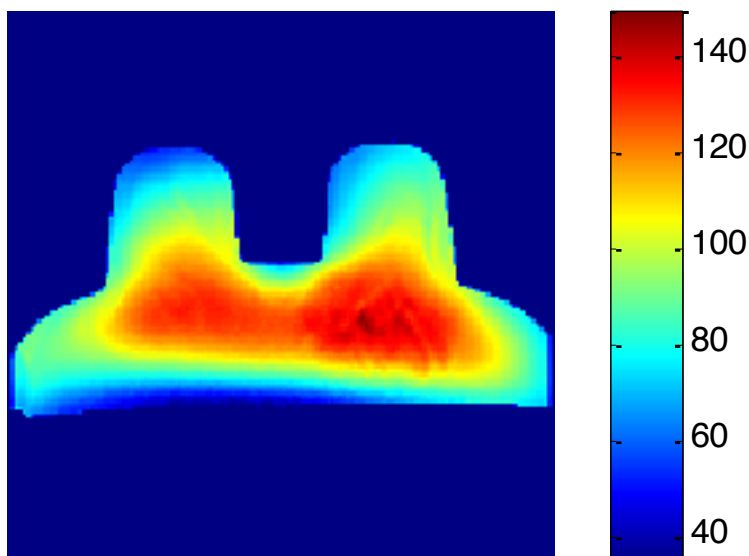
Figure 4. Percent flip angle correction map in flood phantom found by correcting VFA T1 values

With the fat B1 map it is now possible to obtain a B1 map for the whole field of view. To do this we have been testing software to interpolate the missing voxels in the map from the surrounding fat voxels using an inverse distance weighted method. We are testing the accuracy and empirically determining the adequate distance weighting with data from flood phantom scans and volunteer scans. Calculation of fat T1's in patients with a spectroscopic sequence will also continue.

Once the exact methods are nailed down patient specific B1 maps will be calculated for each patient we have scanned, and then T1 and concentration values determined for all cases.

Eleven patients presented for repeated DCEMRI scans at 1.5T and 3T, with the acquisition parameters standardized. Lesion kinetic curves descriptive of the uptake and washout of contrast media were fit to a 3-parameter empirical mathematical model (EMM) (9,10). This was done for percent signal enhancement curves as well as concentration curves calculated with both the linear and non-linear methods (without B1 corrections).

$$SE(t) \ or \ C(t) = \ A(1 - e^{-\alpha t})e^{-\beta t} \quad (1)$$

Where A is the upper limit of signal enhancement (or concentration), α (min^{-1}) is the uptake rate and β (min^{-1}) the washout rate. The EMM parameters provide us with a quantitative estimate of variation in lesion kinetics. In addition to the 3 EMM parameters, maximum measured percent signal enhancement, signal enhancement ratio (SER) (11), and time to peak enhancement (TTP) were also determined for each lesion. TTP was calculated from the EMM parameters – i.e. the time at which Equation 1 is at a maximum. Percent differences were calculated for all the parameters measured by dividing the difference in the value between field strengths by the average of the two.

Conversion to concentration (both linear and non-linear) did not significantly reduce variability in the parameters measured (see Appendix A), likely due to issues with B1 inhomogeneity and native T1 estimation as outlined above.

Table 1 contains the mean values of parameters measured and their differences, for percent signal enhancement curves. A boxplot of the (signed) percent difference is shown in Figure 5. Here the wide range in values for some of the parameters can be visualized. Our results show that TTP and SER had the lowest variability. However, only maximum percent signal enhancement was significantly different between 1.5T and 3T (p = 0.006). Both SER and TTP can be thought of as descriptor of kinetic curve shape, SER relates the early uptake phase to the delayed phase, and TTP depends solely on the uptake and washout rates from the EMM. This is important because curve shape (evaluated qualitatively) is an indicator of malignancy that is routinely used by radiologists. Of the EMM parameters, uptake rate showed the lowest variation, a higher temporal sampling of the uptake phase would likely reduce this variability. Similarly imaging the washout phase longer would also provide more accurate estimates of the rate of washout.

Two radiologists, both experienced in reading breast MRI, evaluated the images and recorded their findings on a 5-point scale. The results of these evaluations can be seen in Table 2. A total image quality score was calculated by adding the scores of the individual criteria. Total image quality at 3T was significantly higher than that at 1.5T (p = 0.005).

Table 1. Measured values of quantitative parameters describing lesion kinetics across all lesions and percent differences between 1.5T and 3T

	Mean value ± std. dev.		Percent	Absolute percent
	1.5T	3T	difference	difference
Max Signal Enhancement[*] (%)	95 ± 32	148 ± 43	43%±30%	45% ± 27%
SER	0.66 ± 0.28	0.68 ± 0.27	7%±34%	22% ± 25%
Enhancement upper limit (A)	219 ± 145	308 ± 208	32%±67%	59% ± 43%
Uptake rate (α) (min^{-1})	0.54 ± 0.45	0.62 ± 0.64	14%±76%	51% ± 55%
Washout rate (β) (min^{-1})	0.06 ± 0.03	0.03 ± 0.03	-11%±84%	67% ± 46%
Time to peak enhancement (min)	5.9 ± 2.7	5.7 ± 2.3	-2%±24%	19% ± 13%

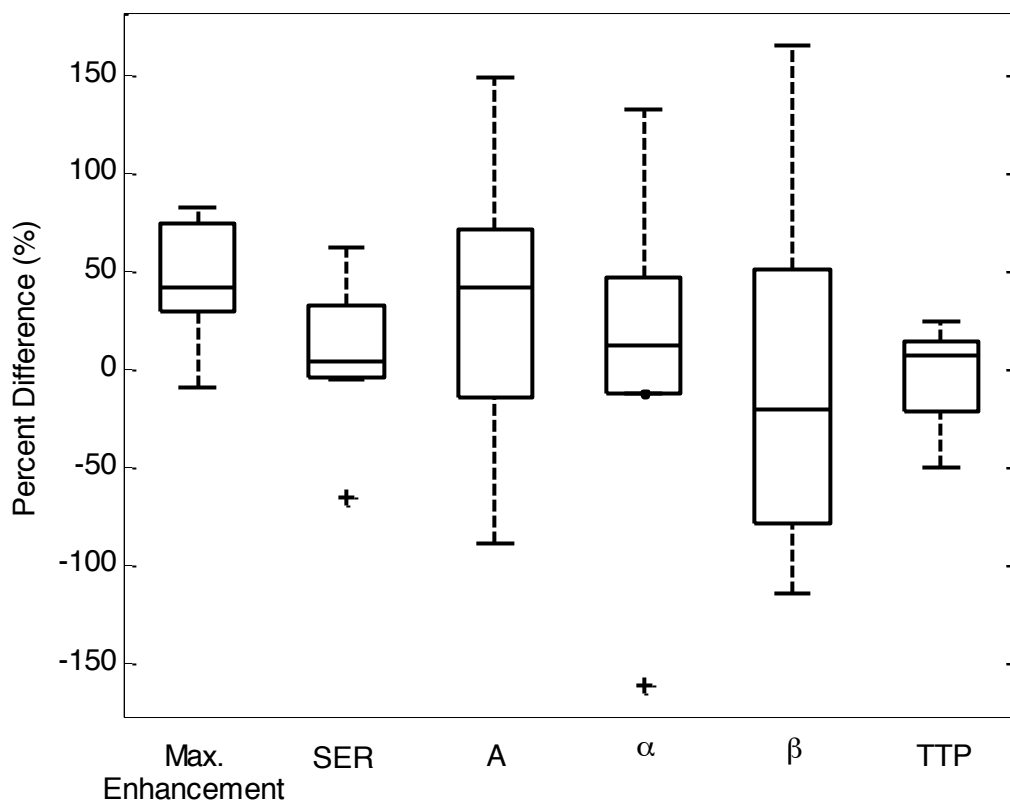* p = 0.006 for comparison between 1.5T and 3T

Figure 5. . Boxplots of signed percent difference between the 1.5T and 3T for all lesions (value measured at 3T minus value measured at 1.5T divided by their average); A, α, β, and TTP are determined from EMM fits. The crosses denote outliers

Table 2. Radiologists' evaluation of image quality

Criterion	Scale[+]		Average rating	
	1	5	1.5T	3T
Total image quality score[*]	**Low**	**High**	**23.4**	**27.7**
Margin sharpness	Low	High	4	4.8
Internal lesion sharpness	Low	High	4	4.9
Lesion conspicuity	Low	High	4.1	5
Fat suppression quality	Poor	Very good	3.9	4.6
Artifact/noise level	High	Low noise	3.7	4.2
Lymph node conspicuity	Low	High	3.7	4.2

+ Total quality score scale ranged from 6 to 30

* p = 0.005

Results from the 1.5T vs. 3T study for signal enhancement parameters will be submitted for publication in the coming weeks. These data will be re-analyzed with the methods described above for conversion to concentration of contrast media.

We have attempted to recruit patients for repeated scans at the same field strength, this would enable us to quantify variability in lesion kinetics not due to changes in field strength but purely due to the physiology and intrinsic uncertainty in our methods. Unfortunately we have been unable to recruit to this study. As an alternative we will look at data from Dr. Olopade's high risk clinic, where women present for MRIs every 6 months, variability in benign lesions present will provide us with an upper bound of variability for lesion kinetics at the same field strength on the same scanner.

A total of 58 women with high-risk breast lesions have been scanned between our group at the UofC and NorthShore. We have created a database with results from the radiological evaluations of the MRI, results of prior imaging studies (mammograms), patient history, biopsy and surgical excision pathology (when available) as well as semi-quantitative parameters from signal enhancement curves and quantitative parameters (determined with the modified methods). Once this database is fully populated we will determine which parameters perform best when ruling out malignancy, providing a potential alternative to surgical management of these breast lesions.

Unfortunately we have been unable to scan women with a hybrid high temporal resolution (for the early phase), and high spatial resolution DCEMRI protocol. Because many of our scans were research add-ons to clinical scans, we were unable to modify the standard DCEMRI portion of the scan. Competition for recruitment between different studies and scanner availability also limited our ability to recruit to a study with a hybrid DCEMRI. Recently we have decided on a

course of action for a pilot study to show the feasibility of such a protocol, if the quality of the images acquired is considered adequate for clinical interpretation recruitment of a larger number of patients will begin.

Key Research Accomplishments

- A total of 62 patients have been scanned at the University of Chicago, and 31 at NorthShore with a research protocol that enables us to measure semi-quantitative and quantitative parameters of lesion kinetics during dynamic contrast enhanced MRI acquisitions.
- We have identified large sources of uncertainty in our quantitative calculations that have been affecting our results, and have come up with a plan to address these issues
- A reference signal method for the estimation of native T1 may increase the accuracy of our estimates as it eliminates dependence on the MRI detectable proton density
- We have found small variability in the measured T1 of fat in the breast, consistent with published results
- As transmit field (B1) inhomogeneity is a large source of error in our calculations, we developed a method using adipose tissue in the breast as a reference, to find patient specific B1 maps
- Analysis of repeated scans of patients at 1.5T and 3T have shown that parameters related to the lesion kinetic curve shape show the least variability of the parameters measured
- We have scanned a total of 58 women with high risk breast lesions and have been putting a database together that will enable us to find parameters that could reliably rule out associated malignancies

Reportable Outcomes

Oral presentations

FD Pineda, M Medved, X Fan, M Ivancevic, H Abe, A Shimauchi, C Sennet, G Newstead, GS Karczmar. "Quantifying variability in DCEMRI of the breast between 1.5T and 3T", presented at the Joint Annual Meeting ISMRM-ESMRMB, Milan, Italy, May 10-16, 2014.

F Pineda, M Medved, X Fan, M Ivancevic, G Newstead, H Abe, C Sennett, G Karczmar. "Quantitative DCE-MRI of the breast at 1.5T and 3T", presented at the 55th Annual Meeting of the AAPM, Indianapolis, IN, August 4-8, 2013.

Poster presentations

M Medved, A Oto, X Fan, **FD Pineda**, RZ Szmulewitz, GS Karczmar. "Differences in Ktrans and ve parameters of gluteal and deep pelvic muscles", presented at the Joint Annual Meeting ISMRM-ESMRMB, Milan, Italy, May 10-16, 2014.

A. Shimauchi, H. Abe, **F. Pineda**, D. Schacht, C. Sennett, G. Newstead, K. Kulkarni. "MR Imaging of Breast before and after Neoadjuvant Chemotherapy: Does Breast Parenchymal Enhancement in the Contralateral Normal Breast Change after Chemotherapy?" presented at the 99th Scientific Assembly and Annual Meeting of the RSNA, Chicago, IL, December 1-6, 2013.

M Medved, A Oto, X Fan, **FD Pineda**, GS Karczmar, RZ Szmulewitz. "Effect of cabozantinib on Ktrans and ve values in castration-resistant prostate cancer", presented at the Joint Annual Meeting ISMRM-ESMRMB, Milan, Italy, May 10-16, 2014.

M. Medved, A. Oto, X. Fan, **F.D. Pineda**, R.Z. Szmulewitz, G.S. Karczmar. "Differences in two-compartment model parameters of gluteal and deep pelvic muscles", presented at the ISMRM 21st Annual Meeting and Exhibition, Salt Lake City, UT, April 20-26, 2013

Manuscripts:

FD Pineda, M Medved, X Fan, MK Ivancevic, H Abe, A Shimauchi, CA Sennett, GM Newstead, GS Karczmar. "Reproducibility of breast lesion kinetic parameters between 1.5T and 3T DCEMRI", to be submitted in April 2014

Conclusions

We continued to scan patients with the full research protocol and with calibration phantoms. 62 patients have been scanned at the University of Chicago and 31 at NorthShore University Healthsystem with the same acquisition parameters (though only patients at this institution were scanned with the calibration phantoms). We have identified the major sources of error in our quantitative methods and have come up with a plan to address them. A novel approach to acquire patient specific B1 maps was developed and has been tested, based on the relatively uniform T1 values of fat in the breast. This approach will correct for what is likely the largest source of uncertainty in our estimates of concentration of contrast media. Further analysis of the 1.5T-3T repeated scans in the same patients has determined that of the parameters measured, two descriptive of lesion kinetic curve shape are the ones which exhibit the lowest variability. These results suggest that descriptors of curve shape may exhibit the highest reproducibility in DCEMRI of the breast. Quantitative analysis of these data may further reduce the variability measured. In the coming weeks the new methods we have developed and tested will be implemented on all the cases acquired. Once this is done we will be able to test the diagnostic accuracy of semi-quantitative and quantitative parameters descriptive of lesion kinetics. Imaging of women with high risk breast lesions has also continued, parameters derived will also be tested as discriminators between benign findings and possible associated malignancies in patients presenting with such lesions, many of which present to surgery for lumpectomy as a standard of care.

References

1. Medved M, Karczmar G. Semiquantitative analysis of dynamic contrast enhanced MRI in cancer patients: variability and changes in tumor tissue over time. J. Magn. … 2004;20:122–8. doi: 10.1002/jmri.20061.

2. Bernstein M, King K, Zhou X. Handbook of MRI Pulse Sequences. In: Elsevier Inc.; 2004. p. 587.

3. Schabel MC, Parker DL. Uncertainty and bias in contrast concentration measurements using spoiled gradient echo pulse sequences. Phys. Med. Biol. 2008;53:2345–73. doi: 10.1088/0031-9155/53/9/010.

4. Rahbar H, Partridge SC, Demartini WB, Gutierrez RL, Parsian S, Lehman CD. Improved B1 homogeneity of 3 Tesla breast MRI using dual-source parallel radiofrequency excitation. J. Magn. Reson. Imaging 2012;35:1222–6. doi: 10.1002/jmri.23571.

5. Azlan C a, Di Giovanni P, Ahearn TS, Semple SIK, Gilbert FJ, Redpath TW. B1 transmission-field inhomogeneity and enhancement ratio errors in dynamic contrast-enhanced MRI (DCE-MRI) of the breast at 3T. J. Magn. Reson. Imaging 2010;31:234–9. doi: 10.1002/jmri.22018.

6. Yarnykh VL. Actual flip-angle imaging in the pulsed steady state: a method for rapid three-dimensional mapping of the transmitted radiofrequency field. Magn. Reson. Med. 2007;57:192–200. doi: 10.1002/mrm.21120.

7. Nehrke K. On the steady-state properties of actual flip angle imaging (AFI). Magn. Reson. Med. 2009;61:84–92. doi: 10.1002/mrm.21592.

8. Rakow-Penner R, Daniel B, Yu H, Sawyer-Glover A, Glover GH. Relaxation times of breast tissue at 1.5T and 3T measured using IDEAL. J. Magn. Reson. Imaging 2006;23:87–91. doi: 10.1002/jmri.20469.

9. Fan X, Medved M, Karczmar GS, Yang C, Foxley S, Arkani S, Recant W, Zamora M a, Abe H, Newstead GM. Diagnosis of suspicious breast lesions using an empirical mathematical model for dynamic contrast-enhanced MRI. Magn. Reson. Imaging 2007;25:593–603. doi: 10.1016/j.mri.2006.10.011.

10. Jansen S, Fan X, Karczmar G. Differentiation between benign and malignant breast lesions detected by bilateral dynamic contrast-enhanced MRI: A sensitivity and specificity study. Magn. … 2008;59:747–54. doi: 10.1002/mrm.21530.

11. Hylton N. Dynamic contrast-enhanced magnetic resonance imaging as an imaging biomarker. J. Clin. Oncol. 2006;24:3293–8. doi: 10.1200/JCO.2006.06.8080.

Appendix A

7478

Quantifying variability in DCEMRI of the breast between 1.5T and 3T

Federico D. Pineda[1], Milica Medved[1], Xiaobing Fan[1], Marko Ivancevic[2], Hiroyuki Abe[1], Akiko Shimauchi[1], Charlene Sennet[1], Gillian Newstead[1], and Gregory S. Karczmar[1]

[1]*Radiology, The University of Chicago, Chicago, IL, United States, *[2]*Philips Healthcare, Netherlands*

TARGET AUDIENCE: Radiologists; medical physicists developing quantitative DCEMRI techniques

PURPOSE: MRI has become a valuable tool in the detection and staging of breast cancer. The enhancement pattern of lesions from a dynamic contrast-enhanced MRI (DCEMRI) acquisition can be a strong indicator of malignancy[1]. However, differences in acquisition parameters and scanner properties can lead to variability in the enhancement pattern seen in lesions. In this study we quantify the variability of parameters related to signal enhancement of lesions in repeated scans of the same patients at two field strengths, 1.5T and 3T. Quantitative analysis of DCEMRI has the potential to provide absolute, standardized measures of kinetic parameters; this requires converting signal intensity to concentration of contrast media. Therefore variability in the data was also assessed after conversion of signal intensity to contrast concentration.

METHODS: Eleven patients were scanned on both Philips Achieva 1.5T and Achieva 3T-TX scanners with 16-channel bilateral breast coils and standardized acquisition protocols under an IRB-approved and HIPAA compliant study. T1-weighted DCEMRI sequences (3D gradient echo) were acquired with 0.8x0.8x1.6mm voxels (interpolated to 0.8mm isotropic), TR/TE = 5/3 ms, FA = 10°, and a temporal resolution of 1min 15s. All patients received a dose of 0.1mM/kg gadodiamide (Omniscan, GE, Waukeesha, WI). Signal intensity time curves were obtained by drawing ROIs over the entire volume of the lesion under radiologist guidance, and then converted to signal enhancement curves expressed in % increase in signal intensity compared to baseline value. Time series were fit to a 3-parameter empirical mathematical model (EMM)[2]. Conversion to contrast agent concentration was performed with both a linear reference signal method, and the non-linear analytic solution to the gradient echo signal model [3,4]. The reference signal used for the linear conversion was from calibration phantoms placed in the breast coil during the acquisition. For the non-linear conversion to concentration, native T1 values were found with a variable flip angle T1-mapping sequence (TR/TE = 10/2.4ms, FA = 5,10,15,20°).

RESULTS: Table 1 contains the mean differences in the EMM parameters between 1.5T and 3T for all 10 lesions present (6 benign, 4 malignant), as well as the time to the maximum enhancement as derived from the EMM. Percent difference was calculated as the subtraction of the parameters at 1.5T and 3T divided by the average of the two. Uptake rate and time to peak enhancement had the lowest variability. Table 2 summarizes the results for maximum signal enhancement, SER and concentration. SER had the lowest variability among these measurements.

EMM Parameter	Signal Enhancement	Linear concentration	Non-linear concentration
Enh./conc. upper limit	64% ± 40%	61% ± 43%	117% ± 52%
Uptake rate	48% ± 57%	51% ± 48%	71% ± 49%
Washout rate	66% ± 49%	98% ± 69%	79% ± 77%
Time to peak	18% ± 14%	35% ± 44%	43% ± 42%

Table 1. Mean differences and standard deviations of EMM parameters between values at 1.5T and 3T

DISCUSSION & CONCLUSIONS: Conversion to concentration did not significantly reduce the variability seen in the measurements based on signal enhancement alone. B1 corrections were not included in concentration measurements; this could account for the increased variability associated with these calculations. In general, linear concentration measurements were less variable than non-linear ones, probably due to errors in estimation of native T1. Time to peak enhancement (derived from the EMM parameters) and SER were the measurements with the lowest variability from the signal time-series, suggesting their importance as primary diagnostic variables. Of the EMM parameters, the uptake rate had the lowest variability. Accrual of more data is ongoing, as well as refinement of measurements including B1 corrections.

	Average value		Average of
	1.5T	3T	differences
Signal Enhancement	86% ± 16%	138% ± 31%	47% ± 29%
SER	0.668 ± 0.293	0.673 ± 0.286	21% ± 27%
Concentration (Linear)	0.17 ± 0.09	0.26 ± 0.22	44% ± 43%
Concentration (Nonlin.)	0.30 ± 0.19	0.70 ± 0.46	83% ± 56%

Table 2. Average maximum values and percent differences for all lesions

1. Kuhl et al., J Magn Reson Imaging 2000; **12**: 965
2. Fan et al., Magn Reson Imaging 2007; **25**:593
3. Medved, et al., J Magn Reson Imaging 2004, **20**: 122.
4. Schabel, et al., Phys. Med. Biol. 2008, **53**: 2345